

The modular structure of dovyrenite, $\text{Ca}_6\text{Zr}[\text{Si}_2\text{O}_7]_2(\text{OH})_4$: Alternate stacking of tobermorite and rosenbuschite-like units

MILEN KADIYSKI,^{1,*} THOMAS ARMBRUSTER,¹ EVGENY V. GALUSKIN,² NIKOLAY N. PERTSEV,³
ALEKSANDER E. ZADOV,⁴ IRINA O. GALUSKINA,² ROMAN WRZALIK,⁵ PIOTR DZIERZANOWSKI,⁶ AND
EVGENY V. KISLOV⁷

¹Mineralogical Crystallography, Institute of Geological Sciences, University of Bern, Freiestr. 3, CH-3012 Bern, Switzerland

²Faculty of Earth Sciences, Department of Geochemistry, Mineralogy and Petrography, University of Silesia, Bedzinska 60, 41-200 Sosnowiec, Poland

³Institute of Geology of Ore Deposits, Geochemistry, Mineralogy and Petrography (IGEM) RAS, Staromonetny 35, Moscow, Russia

⁴Sci.-Research Center “NEOCHEM,” Altuf’evskoye Highway 43, Moscow, Russia

⁵Institute of Geochemistry, Mineralogy and Petrology, Warsaw University, al. Zwirki i Wigury 93, 02-089 Warszawa, Poland

⁶Institute of Geology, Siberian Branch, RAS, Sakhyanova Str. 6, 670042 Ulan-Ude, Russia

⁷Institute of Physics, University of Silesia, Uniwersytecka 12, 41-200 Katowice, Poland

ABSTRACT

The average structure, space group *Pnmm* [subcell: $A = 5.666(16)$, $B = 18.844(5)$, $C = 3.728(11)$ Å, $V = 398.0(2)$ Å³, $Z = 1$], of the new mineral dovyrenite $\text{Ca}_6\text{Zr}[\text{Si}_2\text{O}_7]_2(\text{OH})_4$ has been refined from single-crystal X-ray data to $R = 7.97\%$. The modular structure of dovyrenite is built by alternate stacking of Ca-polyhedral layers characteristic of the tobermorite structure and octahedral layers with attached disilicate groups known from the rosenbuschite group of minerals. No indications of ordered polytypes were detected for the potential OD-structure. Either the small crystal size producing only weak diffraction intensities did not allow detecting diffuse diffraction features (or “super-structure” reflections) or the structure is built by disordered stacks of OD layers. Nevertheless, the resolved average structure allowed unraveling the possible order patterns within the rosenbuschite-like octahedral layers. The key for understanding the polytypic character of this structure is the short periodicity of the tobermorite-like Ca polyhedral layer of only 3.73 Å along *c*, whereas the periodicity of the attached rosenbuschite-like octahedral layer is doubled. In dovyrenite Ca occurs in sixfold-, sevenfold-, and eightfold-coordination. The octahedral Ca site is only half occupied and may reveal additional vacancies, which must be charge balanced by disordered OH-groups replacing O. A corresponding modular structure with the same subunits but different composition and without octahedral vacancies exists for rinkite $(\text{Ti}, \text{Nb}, \text{Al}, \text{Zr})(\text{Na}, \text{Ca})_3(\text{Ca}, \text{Ce})_4[\text{Si}_2\text{O}_7]_2(\text{O}, \text{F})_4$, which has hitherto been considered as heterophyllosilicate.

Keywords: Dovyrenite, zirconosilicates, single-crystal X-ray diffraction, structure solution, modular structure, tobermorite, rinkite, heterophyllosilicate

INTRODUCTION

Ferraris et al. (2004) begin their book on crystallography of modular materials citing a phrase by Galileo Galilei: “Nature does not act by means of many things when it can do so by means of few.” This is also particularly true for the crystal structure of the new mineral dovyrenite $\text{Ca}_6\text{Zr}[\text{Si}_2\text{O}_7]_2(\text{OH})_4$, assembled of two well-known modules characteristic of the polyhedral Ca-sheet in tobermorite group minerals and the octahedral layer with attached disilicate moieties of the rosenbuschite group. Minerals of the rosenbuschite group are disilicates with the crystal-chemical formula $\text{M}_6[\text{Si}_2\text{O}_7]_4(\text{O}, \text{OH}, \text{F})_8$, comprising the minerals götzenite, seidozerite, rosenbuschite, hainite, kochite, and grenmarite (Bellezza et al. 2004), whereas minerals of the tobermorite group are hydrated calcium silicates characterized by wollastonite-like chains of SiO_4 tetrahedra connected to sheets

of sevenfold-coordinated calcium cations (Taylor 1959; Merlino et al. 1999, 2000, 2001).

A remarkable coincidence is the similarity of the subcell dimensions and symmetry between riversideite $\text{Ca}_5[\text{Si}_6\text{O}_{16}(\text{OH})_2] \times n\text{H}_2\text{O}$ (tobermorite 9 Å) and dovyrenite. In standard space-group setting *Pnmm* dovyrenite has $A = 5.67$, $B = 18.84$, $C = 3.73$ Å, whereas riversideite has $A = 5.58$, $B = 18.70$, $C = 3.66$ Å (Taylor 1959; Ferraris et al. 2004), although the true structures and chemical compositions show important differences. The definition and description of dovyrenite as a new mineral will be published elsewhere (Galuskin et al. 2007). This manuscript deals with the analysis and interpretation of the modular structure of the new mineral (accepted by CNMMN IMA 2007-002).

OCCURRENCE

The new mineral dovyrenite was discovered in altered skarn-dolomite xenoliths in the Dovyren (Yoko-Dovyren) subvolcanic layered gabbro-peridotite massif of Proterozoic Age (~700 Ma)

* E-mail: kadiyski@krist.unibe.ch

located 60 km north of Baikal Lake, 56.5° N and 110° E (Gurulev 1983; Konnikov 1986; Kislov 1998; Wenzel et al. 2002; Pertsev et al. 2003; Zadov et al. 2004). The skarn-dolomite xenoliths in the dunite and troctolite layers trace the position throughout the magmatic body of the host dolomite-bed replaced by magma.

Dovyrenite is associated with foshagite, vesuvianite, pyroxene of the series diopside–Al–Ti–diopside (“fassaitite”), monticellite, calzirtite, tazheranite, baghdadite, perovskite, apatite, calcite, brucite, melilite, and forsterite. In addition, rare crystals of $\text{Ca}_8\text{Zr}(\text{Si}_2\text{O}_7)_2(\text{CO}_3)_2(\text{OH})_4$ associated with dovyrenite represent a potential new mineral species.

Dovyrenite formed at the regressive stage of early magmatic skarn formation as an alteration product of Zr-bearing and zirconium minerals. Dovyrenite occurs within the central skarn zone in xenoliths (up to a few centimeters in thickness and 10–20 cm in length) composed of dark-brown titanian-fassaitic pyroxene. Postmagmatic processes liberated Ti and Zr from pyroxene leading to newly formed perovskite, calzirtite, tazheranite, baghdadite, and dovyrenite. Dovyrenite crystallized as the last phase frequently forming pseudomorphs after calzirtite. Coexistence of foshagite and monticellite in the same rock indicates a narrow temperature range for dovyrenite crystallization at 590–630 °C under shallow conditions ($P < 1$ kbar) of skarn formation (Pertsev et al. 2003; Zadov et al. 2004).

EXPERIMENTAL METHODS

For the structure analysis, a crystal of $\text{Ca}_8\text{Zr}(\text{Si}_2\text{O}_7)_2(\text{OH})_4$, ca. $0.10 \times 0.02 \times 0.01$ mm³ in size was mounted on a Bruker PLATFORM three circle goniometer equipped with an 1K SMART CCD detector with a crystal-to-detector distance of 5.4 cm. Data were collected using graphite monochromated $\text{MoK}\alpha$ ($\lambda = 0.71073$ Å) radiation and frame widths of 0.3° in ω , with 360 s used to acquire each frame. As subsequent structure refinement indicated (see below), all observed reflections had to be considered family reflections of possible polytypic series. Thus, only subcell dimensions [$A = 5.666(16)$, $B = 18.844(5)$, $C = 3.728(11)$ Å, $V = 398.0(2)$

TABLE 1. Parameters for X-ray data collection and crystal structure refinement

Diffractometer	Siemens Smart CCD 1K
X-ray radiation	$\text{MoK}\alpha$ (0.71073 Å)
X-ray power	50 kV, 40 mA
Temperature (K)	293
Crystal size (mm)	$0.1 \times 0.02 \times 0.01$
Detector to sample distance (cm)	5.4
Rotation axis	ω
Rotation width	0.3°
Total number of frames	1362
Frame size	512×512 pixels
Time per frame	360 s
Space group	<i>Pnmm</i> (no. 58)
Cell dimensions (Å)	5.666(16), 18.844(5), 3.728(11)
Cell volume (Å ³)	398.0(2)
Z	1
Collection mode	automated hemisphere
Reflections collected	2306
Max. 2 θ	56.5
Index range	$-26 \leq h \leq 26$; $-2 \leq k \leq 6$; $-14 \leq l \leq 15$
Unique reflections	523
Reflections > 2 $\sigma(I)$	432
R_{int}	0.0856
R_{σ}	0.0605
Number of least squares parameters	59
Goof	1.477
$R1$, $I > 2\sigma(I)$	0.0797
$R1$, all data	0.1201
$wR2$ (on F^2)	0.1840
$\Delta\rho_{\text{min}}$ (–e. Å ^{–3})	1.4 (1.6 Å from O5)
$\Delta\rho_{\text{max}}$ (e. Å ^{–3})	1.2 (1.6 Å from O5)

Å³, $Z = 1$) of an average structure could be determined (Table 1).

When it was recognized that the recorded intensity data were characteristic of family reflections of a polytypic series, we systematically searched for evidence of additional reflections, marking the presence of ordered polytypes or diffuse diffraction features that would be indicative of partial disorder. However, such evidence was not found. A total of 2306 reflections of a hemisphere in reciprocal space were collected up to $2\theta = 56.08^\circ$ at room temperature. Data were reduced and corrected for Lorentz, polarization, and background effects using the program SAINT (Bruker 1999). Scattering curves for neutral atoms, together with anomalous dispersion corrections, were taken from *International Tables for Crystallography*, vol. C (Wilson 1992). The Bruker SHELXTL Version 5.1 (Bruker 1997) system of programs was used for the refinement of the crystal structure on the basis of F^2 , using 523 unique reflections, with 432 classified as observed ($F_o > 4\sigma F_o$). The reflection statistics and systematic absences were found to be consistent with space groups *Pnmm* and *Pnn2*. Subsequent attempts to solve the structure indicated that the observed average structure is centrosymmetric and for this reason *Pnmm* (no. 58) is the correct space group. Direct methods were utilized to locate the atoms Ca1 and Ca2. By subsequent difference-Fourier summations the oxygen atoms O1 to O5, X3, and Si1 were found. The positions of Ca2, O4, O5, and Si1 are half occupied due to the observed average structure. X3 contains 0.5 Ca (Ca3) and 0.5 Zr (Zr3). Finally, four [OH][–] groups per formula unit (O2 position) were assigned by calculation of the bond valences, using VALENCE 1.0 program (Brown and Altermatt 1985). The small crystal size and the associated low diffraction intensities did not allow for determination of H⁺ positions. Least squares refinement of all atom-position parameters, allowing for anisotropic displacement of all atoms, and the inclusion of a weighting scheme of the structure factors, resulted in a final agreement index ($R1$) of 0.0797, calculated for the unique observed reflections.

RESULTS

Results from electron microprobe analysis are given in Table 2. The final atom parameters are listed in Table 3, anisotropic atomic displacement parameters are presented in Table 4 and in CIF data set¹. Results of bond valence calculations using the constants of Brown and Altermatt (1985) are summarized in Table 5. Due to the average character of the structure, bond valence calculations cannot be as accurate as they would be for an ordered polytype. Selected interatomic distances and bond angles are listed in Table 6.

¹ Deposit item AM-08-011, CIF data set. Deposit items are available two ways: For a paper copy contact the Business Office of the Mineralogical Society of America (see inside front cover of recent issue) for price information. For an electronic copy visit the MSA web site at <http://www.minsocam.org>, go to the American Mineralogist Contents, find the table of contents for the specific volume/issue wanted, and then click on the deposit link there.

TABLE 2. Composition of dovyrenite crystals from foshagite-vesuvianite skarn, Dovyren Massif, Russia

Oxide	Dovyrenite	e.s.d.	Range	Element	apfu
	average of 13				
ZrO ₂	16.64	0.28	16.21–17.25	Zr	0.990
SiO ₂	32.78	0.18	32.45–33.09	Si	4
TiO ₂	0.05	0.06	0–0.17	Ti ⁴⁺	0.005
HfO ₂	0.12	0.03	0.07–0.17	Hf	0.004
CaO	43.90	0.42	43.21–44.46	Ca	5.739
FeO	0.27	0.07	0.14–0.38	Fe ²⁺	0.028
MgO	0.13	0.04	0.06–0.22	Mg	0.024
MnO	0.02	0.03	0–0.07	Mn ²⁺	0.002
Nb ₂ O ₅	0.03	0.04	0–0.08	Nb ⁵⁺	0.002
H ₂ O	5.42	0.17	5.1–5.7	OH	4.412
Total	99.36		98.96–100.09	O	13.588

Notes: Formula calculated on the basis of 4 Si. EMPA CAMECA SX100: 15 kV, 0–20 nA, spot 3–10 μm. Analytical lines and standards: ZrL α = zircon, ZrO₂; CaK α , SiK α , MgK α = diopside; TiK α = rutile; CrK α = Cr₂O₃ syn.; HfM β = Hf-SPY; YL α = YAG; AlK α = orthoclase; FeK α = Fe₂O₃ syn.; MnK α = rhodochrosite; NbL α , VK α = pure metal. Elements F, Ta, B, Na, K, etc. not detected. PAP-correction.

Structural features

The refined model corresponds to the average structure of this new mineral. Half occupancies allow for different possible arrangements in the true structure. The fact that we did not observe any diffraction evidence indicating ordered polytypes suggests two possible interpretations: (1) the structure exhibits long-range disorder or (2) there are several ordered polytypes but evidence of these polytypes could not be found due to the small crystal size and the expected weak intensity of additional reflections associated with the presence of polytypic order.

In dovyrenite, Ca is found to exist on three independent sites, being sixfold-, sevenfold-, and eightfold-coordinated, named Ca2, Ca1, and Ca3, respectively. The structure may be described as built up by the following components: (1) infinite layers, perpendicular to **b**, formed by sevenfold-coordinated Ca1 polyhedra, which are arranged in columns running along **c** (Fig. 1). These layers are topologically equivalent to those found in the tobermorite group of minerals (Hoffmann and Armbruster 1997; Merlino et al. 1999, 2000, 2001). Those Ca1 polyhedra are edge connected to adjacent Ca1 polyhedra building a fully occupied Ca-O layer, which expands infinitely in the **ac** plane, stacked along **b**. The sevenfold Ca1 coordination polyhedron has a pyramidal part on one side and a dome part on the other side. These polyhedra are connected in such fashion that every second polyhedron has its pyramidal part pointing up, thus the layer undulates along the **a** axis (Figs. 1 and 3). The topological periodicity of this (010) layer corresponds to the observed periodicity (*A* and *C*) of the average structure; and (2) in the

observed average structure Zr3 (occupancy 50%) and Ca3 (occupancy 50%) occupy the same site X3, where X3 forms infinite chains of edge-sharing polyhedra expanding along **c** (Fig. 2). However, there is clear evidence that in the true structure Zr3 and Ca3 have to alternate along the **c** axis. Alternation between these polyhedra is indicated by splitting of the O4 positions, which form the connecting polyhedral edge and which are not situated on the mirror plane perpendicular to **c**. Thus parallel to the **c** axis large polyhedra (Ca3) have to alternate with small polyhedra (Zr3). This gives rise to two possible arrangements of these polyhedra, since every Zr3 octahedron could take the place of a Ca3 polyhedron and vice versa.

Above and below (along **b**) the infinite X3 chains there are disilicate $[\text{Si}_2\text{O}_7]^{6-}$ groups (occupied to 50%) attached to X3 polyhedra by sharing apices. Oxygen O5 (50% occupied) represents the bridging oxygen between two Si tetrahedra. There must be short-range order of these disilicate groups to avoid short Si-Si distances of ca. 0.8 Å. Thus there is an alternation along **c** of occupied and empty disilicate units leaving the choice of whether $[\text{Si}_2\text{O}_7]^{6-}$ groups “crown” Zr3 or Ca3 polyhedra. To maintain optimum tetrahedral geometry (regular bond lengths and low angular O-T-O distortions) disilicate groups can only be associated with Ca3 polyhedra where the bridging O5 expands the Ca3

TABLE 3. Atom coordinates, occupancies, and isotropic displacement parameters for dovyrenite

Atom	<i>x</i>	<i>y</i>	<i>z</i>	U_{eq}	Occupancy
Ca1	0.1796(5)	0.1958(14)	0.0000	0.0114(7)	1.0
Ca2	0.5000	0.5000	0.0000	0.0170(4)	0.358(18)
X3	0.0000	0.5000	-0.5000	0.0156(7)	0.5 Ca + 0.5 Zr
Si	0.1699(8)	0.3593(2)	0.0703(12)	0.0102(18)	0.50
O1	-0.0497(16)	0.3081(5)	0.0000	0.0140(2)	1.0
O2	0.1730(2)	0.0636(5)	0.0000	0.0300(3)	1.0
O3	0.4153(16)	0.3204(5)	0.0000	0.0140(2)	1.0
O4	0.1480(2)	0.4389(6)	0.1060(3)	0.0160(3)	0.50
O5	0.1560(4)	0.3807(11)	0.5000	0.0250(5)	0.50

TABLE 4. Anisotropic atomic displacement parameters for dovyrenite

Atom	U_{11}	U_{22}	U_{33}	U_{23}	U_{13}	U_{12}
Ca1	0.0116(13)	0.0160(13)	0.0065(12)	0.0000	0.0000	0.0025(11)
Ca2	0.0080(5)	0.0310(6)	0.0120(5)	0.0000	0.0000	-0.0070(5)
X3	0.0238(14)	0.0063(11)	0.0166(13)	0.0000	0.0000	0.0015(11)
Si	0.0140(2)	0.0086(19)	0.0080(5)	0.0015(16)	-0.0023(18)	0.0026(17)
O1	0.0190(5)	0.0150(4)	0.0090(4)	0.0000	0.0000	0.0000(4)
O2	0.0490(7)	0.0120(5)	0.0310(6)	0.0000	0.0000	-0.0010(5)
O3	0.0120(4)	0.0140(4)	0.0150(5)	0.0000	0.0000	0.0040(3)
O4	0.0230(7)	0.0120(5)	0.0150(7)	-0.0100(4)	0.0000(5)	-0.0080(5)
O5	0.0310(12)	0.0250(11)	0.0190(10)	0.0000	0.0000	0.0190(10)

TABLE 5. Results of bond valence calculations of an ordered variety* using the constants of Brown and Altermatt (1985)

	O1	O2	O3	O4	O5	Total
Ca1	0.297(x2) 0.250	0.241	0.330(x2) 0.138			1.883
Ca2		0.293(x4)↔		0.370(x2)↔		1.912
Ca3		0.522(x2)↔		0.151(x4)↔	0.296(x2)↔	2.240
Si1	1.125		1.133	0.989	0.966(x2)↓	4.213
Zr3		0.470(x2)↔		0.728(x4)↔		3.852
Total	1.969	1.056(Ca3) 1.004(Zr3)	1.931	2.238	2.228	

Notes: Arrows represent the direction in which the multiplier (in brackets) should be taken into account.

* Ca3 and Zr3 (X3) are assumed to alternate along the **c** axis. Ca and vacancies on Ca2 (half occupied) are assumed to alternate along **c**.

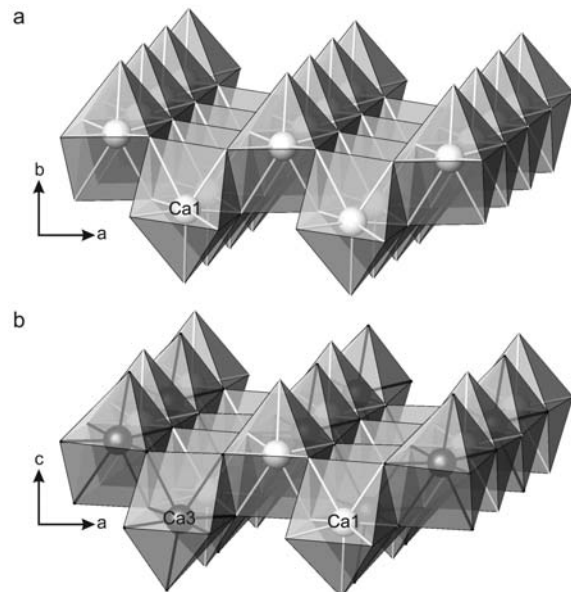


FIGURE 1. (a) The layer of sevenfold-coordinated Ca in dovyrenite and (b) in clinotobermorite 9 Å (Merlino et al. 2000). Black and white spheres represent symmetrically non-equivalent Ca structure sites.

TABLE 6. Selected interatomic distances and bond angles for dovyrenite

Ca1-O3 (2×)	2.411(6)	Zr3-O4 (4×)	2.050(1)
Ca1-O1 (2×)	2.417(6)	Zr3-O2 (2×)	2.210(1)
Ca1-O1	2.480(1)	Mean	2.100
Ca1-O2	2.490(1)		
Ca1-O3	2.700(1)	Si-O1	1.600(1)
Mean	2.475	Si-O3	1.590(1)
		Si-O4	1.640(1)
Ca2-O4 (2×)	2.330(1)	Si-O5	1.653(7)
Ca2-O2 (4×)	2.421(7)	Mean	1.621
Mean	2.381		
		O1-Si-O3	111.8(6)
Ca3-O4 (4×)	2.670(1)	O1-Si-O4	115.5(6)
Ca3-O2 (2×)	2.210(1)	O4-Si-O3	115.0(3)
Ca3-O5 (2×)	2.420(2)	O1-Si-O5	105.5(9)
Mean	2.490	O4-Si-O5	99.3(8)
		O3-Si-O5	108.3(8)
		Si-O5-Si	151.0(1)

polyhedron from octahedral to eightfold coordination.

Ca2 octahedra fill interstices between the chains of alternating Zr3 and Ca3 polyhedra. As mentioned above, Ca2 has half occupancy to maintain the observed stoichiometry $\text{Ca}_6\text{Zr}[\text{Si}_2\text{O}_7]_2(\text{OH})_4$. This leaves the choice of whether Ca2 octahedra exhibit short-range order by alternation of occupied and vacant sites or whether there is occupational disorder. The answer on this question is obtained by bond-valence calculations, suggesting an ordered occupational model to avoid irregular oxygen bond-valences. As an example, with regular alternate occupation of Ca2 each O2 site would bond once to Ca2 yielding an O2 bond valence of 1.0 as characteristic of an OH group. If the Ca2 octahedra were randomly occupied, some O2 sites would bond twice to Ca2 (the O2 bond valence increases by 0.24), whereas other O2 sites would not bond Ca2 (the O2 bond valence decreases by 0.24). According to the least square refinements, the occupancy of Ca2 site is even less than half (Table 3). These additional Ca2 vacancies must be charge balanced by (disordered) OH-groups replacing O. The occupancy of Ca2 would be half only for the stoichiometric $\text{Ca}_6\text{Zr}[\text{Si}_2\text{O}_7]_2(\text{OH})_4$ composition.

A module consisting of a sheet of octahedra with attached disilicate moieties found in dovyrenite is not new but has been already identified in the structure of the rosenbuschite group of minerals (Bellezza et al. 2004). However, in rosenbuschite-group minerals the octahedral site corresponding to Ca2 in dovyrenite is completely occupied. Furthermore, in rosenbuschite the fashion in which the disilicate moieties are attached to the sheet of octahedra can be described by a twofold axis along **b** (Fig. 2c), the extension direction of chains within the layer (corresponding to **c** in dovyrenite). This strictly defined arrangement of disilicate moieties in rosenbuschite is a consequence of the diagonal **b**-extending ribbons of octahedra (Bellezza et al. 2004) interconnecting the sheets of octahedra. In dovyrenite a modified arrangement of disilicate moieties is possible where these disilicate groups follow a staggered fashion, described by a 2_1 axis parallel to **c**, the extension of chains of edge-sharing octahedra.

The linkage of the rosenbuschite-like octahedral sheet with the Ca polyhedral layer, characteristic of tobermorite, is accomplished via the disilicate groups. Si tetrahedra in dovyrenite are edge-connected to the dome parts of the sevenfold-coordinated Ca1 in the tobermorite undulated layers. The Si-O distances are

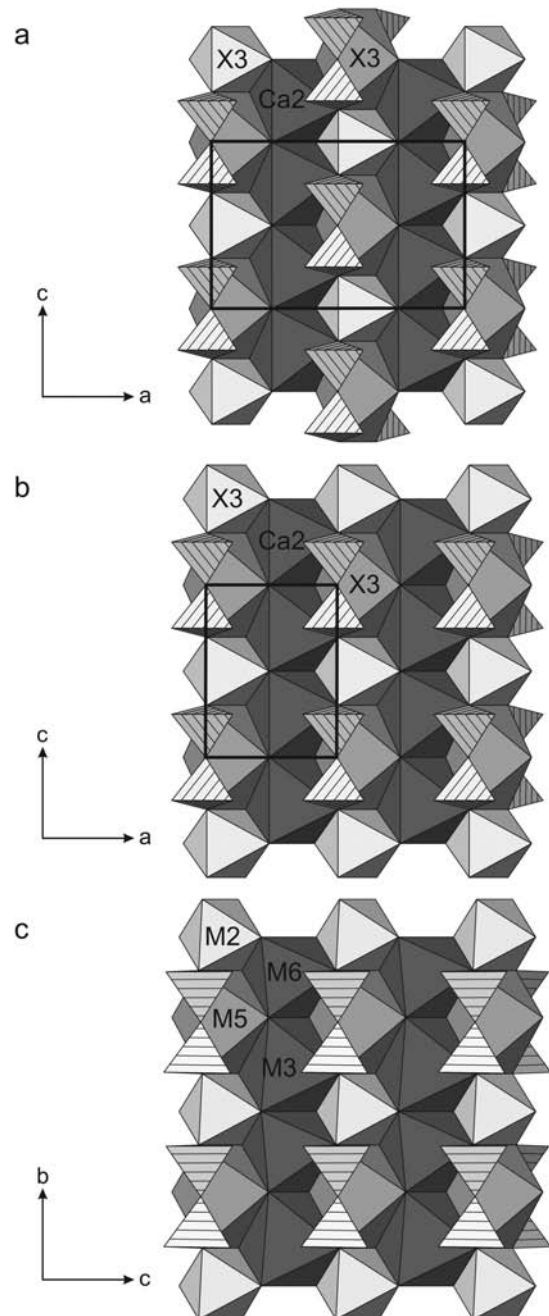


FIGURE 2. Possible arrangements of disilicate units (dashed) in the “rosenbuschite-like” layer in dovyrenite (**a**, **b**), viewed along [010] and in grenmarite (**c**), viewed along [100] (Bellezza et al. 2004). The X3 site in dovyrenite is alternately occupied by Ca and Zr; in grenmarite M2 is occupied by (Zr, Mn); M3 by (Mn, Ca); M5 and M6 by (Ca, Na).

between 1.59 and 1.65 Å, where the longest distance Si-O5 of 1.65 Å is due to the Si-O5-Si bridging angle of 151°. Lengthening of the Si-O5 distance is in agreement with findings of Gibbs (1982) based on molecular orbital calculations for disilicate groups. In rosenbuschite group of minerals Si-O-Si angles vary between 154 and 173° depending on the size and occupancy of octahedral sites connected to the disilicate moieties (Bellezza

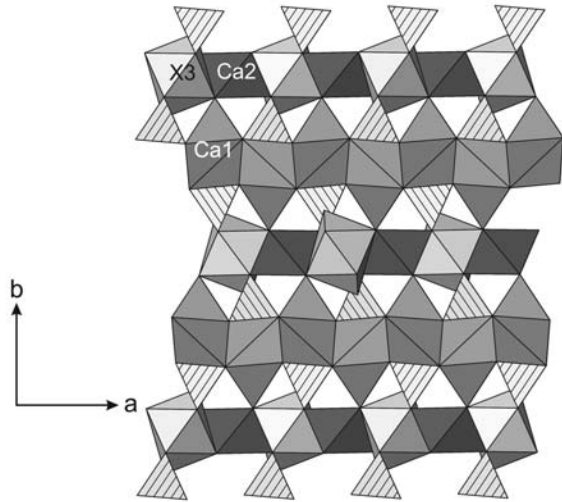


FIGURE 3. Polyhedral model of the structure of dovyrenite, viewed along [001]. SiO_4 tetrahedra are hatched; Ca3 on X3 sites are drawn with their true eightfold coordination.

et al. 2004).

For the structural model discussed above any long-range ordered polytype must have a doubled C axis ($c = 7.456 \text{ \AA}$) due to alternation of ZrO_6 and CaO_6 octahedra with attached disilicate groups. In the model with staggered Ca3-Zr3 chains, it is obvious that not only C but also the A -axis must be doubled yielding $a = 11.332$, $b = 18.844$, and $c = 7.456 \text{ \AA}$ and a B -centered lattice.

An alternative model would be short-range ordered layers, leading to a long-range disordered structure. This would happen if, e.g., in subsequent layers, ordered Zr3 and Ca3 polyhedra are shifted 3.728 \AA ($1 \times C$) along c . This type of occupational stacking disorder is comparable with the completely Si, Al ordered sheets discussed for kinoshitalite $\text{BaMg}_3(\text{Al}_2\text{Si}_2)\text{O}_{10}(\text{OH},\text{F})_2$ (Gnos and Armbruster 2000) yielding a long-range disordered structure with only one tetrahedral site (characteristic of 50% Si and 50% Al) due to stacking disorder of fully Si, Al ordered sheets of tetrahedra.

Comparison with tobermorite 9 Å (riversideite) or clinotobermorite 9 Å

As mentioned in the introduction section dovyrenite and riversideite possess the same space group for the average structure and reveal also very similar cell dimensions, which needs to be discussed (Fig. 4). Both structures have the tobermorite-like layer of Ca polyhedra in common but are distinct in the way that two adjacent Ca polyhedral layers are linked.

The exact structure of riversideite is actually not known but may be derived from those of “clinotobermorite-9 Å” and “tobermorite-9 Å” (Ferraris et al. 2004). If heated above $300 \text{ }^\circ\text{C}$, both clinotobermorite-11 Å and tobermorite-11 Å dehydrate and simultaneously double chains decondensate to single chains of wollastonite type reducing the stacking distance between adjacent Ca-polyhedral layers from 11 to 9 Å. It is assumed (Ferraris et al. 2004) that riversideite and “clinotobermorite-9 Å” are built by the same OD layers.

Thus in riversideite the connection between two adjacent

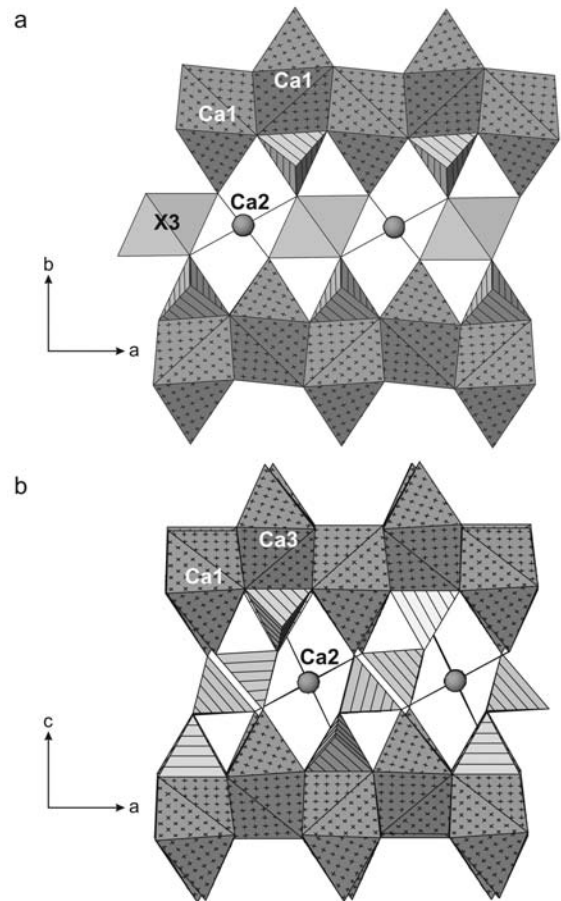


FIGURE 4. Fragment of the structure of (a) dovyrenite and (b) clinotobermorite 9 Å and riversideite (Merlino et al. 2000) indicating their strong similarity. The crossed pattern characterizes the tobermorite sheet of sevenfold-coordinated Ca (see Fig. 1); tetrahedra are hatched.

Ca polyhedral layers is established by wollastonite-like chains of tetrahedra, whereas in dovyrenite a rosenbuschite-like layer of octahedra with attached disilicate groups connects the Ca-polyhedral layers. The wollastonite-like chain of tetrahedra in riversideite may be divided into paired $[\text{Si}_2\text{O}_7]^{6-}$ tetrahedra, edge-sharing with the sevenfold-coordinated Ca polyhedra, and a “bridging” tetrahedron that shares the capping oxygen of the adjacent Ca polyhedral layer. Dovyrenite has the paired tetrahedra (disilicate groups) as found in riversideite but in dovyrenite these pairs are not connected by a linking tetrahedron but by a chain of alternating $[\text{ZrO}_6]$ and $[\text{CaO}_6]$ octahedra. In projections of dovyrenite parallel to c a twofold axis parallel to the octahedral chain looks very similar to a 2_1 parallel to b in riversideite, responsible for the stacking of the wollastonite like chains of tetrahedra. In the average structure of riversideite the 2_1 becomes a 2, which makes the space groups identical for the two substructures.

The rinkite group of minerals

The observed modular structure is not unique to dovyrenite but has been observed before for rinkite, $(\text{Ti},\text{Nb},\text{Al},\text{Zr})(\text{Na},\text{Ca})_3(\text{Ca},\text{Ce})_4[\text{Si}_2\text{O}_7]_2(\text{O},\text{F})_4$ (Galli and Alberti 1971; Rasts-

vetaeva et al. 1991). However, at the time of the rinkite structure refinements the true nature of tobermorite-group minerals was not established and for this reason the modular aspect did not become apparent.

Judging from chemical composition and unit-cell dimensions, nacareniobsite-(Ce) with an idealized end-member formula $\text{NbNa}_3\text{Ca}_3\text{REE}[\text{Si}_2\text{O}_7]_2\text{OF}_3$ (Petersen et al. 1989) seems to be an additional representative of the rinkite group. Rinkite and nacareniobsite-(Ce) are, apart from the chemical composition, distinct to dovyrenite because the former two minerals have no extended vacancies in the octahedral sheet. However, both minerals have a pronounced orthorhombic substructure of ca. $A = 18.46$, $B = 5.67$, $C = 3.72$ Å (Gottardi 1966; Petersen et al. 1989) in common with dovyrenite.

Possible evidence for OD-type polytypism has been noted by Petersen et al. (1989) recording single-crystal diffraction photographs of rinkite. They report diffuse diffractions “probably because of the presence of several individuals.” In a similar context Galli and Alberti (1971) state that $23\bar{1}$ and $44\bar{1}$ reflections were ignored because the background was anomalously high. The high background may be re-interpreted as evidence of diffuse scattering. Christiansen and Rønsbo (2000) discuss possible OD features in rinkite and conclude that a polytypic structure to rinkite, with uniform octahedral sheets, may also exist. Comparison of the structural data on rinkite indicates that the stacking arrangement found by Li et al. (1965) for a pseudo-orthogonal cell setting with $a = 18.3$, $b = 5.6$, $c = 7.4$ Å, $\beta = 90^\circ$, space group $P2_1$, is different from the stacking found in all other studies using a monoclinic unit cell of ca. $a = 7.4$, $b = 5.7$, $c = 18.8$ Å, $\beta = 101^\circ$ (Simonov and Belov 1968; Galli and Alberti 1971; Rastsvetaeva et al. 1991). However, Simonov and Belov (1968) cast some doubts on the correctness of the pseudo-orthogonal structure by Li et al. (1965) because the coordinates could not be refined. Instead, Simonov and Belov (1968) present a monoclinic structure with $\beta = 101^\circ$. Structure refinements using the $\beta = 101^\circ$ setting were performed either in space group $P2_1$ or $P2_1/c$. The choice of space group does not influence the topology of the structure but space group $P2_1$ allows for additional cation order, in particular within the tobermorite-like module. In Table 7, the cation site assignment in $P2_1$ (Rastsvetaeva et al. 1991) and $P2_1/c$ rinkite (Galli and Alberti 1971) is compared with dovyrenite.

Rinkite and dovyrenite interpreted as heterophyllosilicates

Several authors consider rinkite and, consequently also dovyrenite, as members of the heterophyllosilicates or at least

related to them. Structures of this group are formed by an octahedral sheet (O-sheet) alternating with a sheet (H-sheet) containing Si and additional metal cations (Christiansen and Rønsbo 2000). In the more stringent definition by Ferraris et al. (1997, 2004) the H-sheet (hetero) contains a row of Ti^{4+} polyhedra substituting for a row of disilicate tetrahedra in a tetrahedral sheet that is typical of layer silicates. Thus, according to Ferraris et al. (1997, 2004) rinkite and dovyrenite are only structurally related (plesiotypes) to heterophyllosilicates because there is no Ti^{4+} or Zr^{4+} substitut-

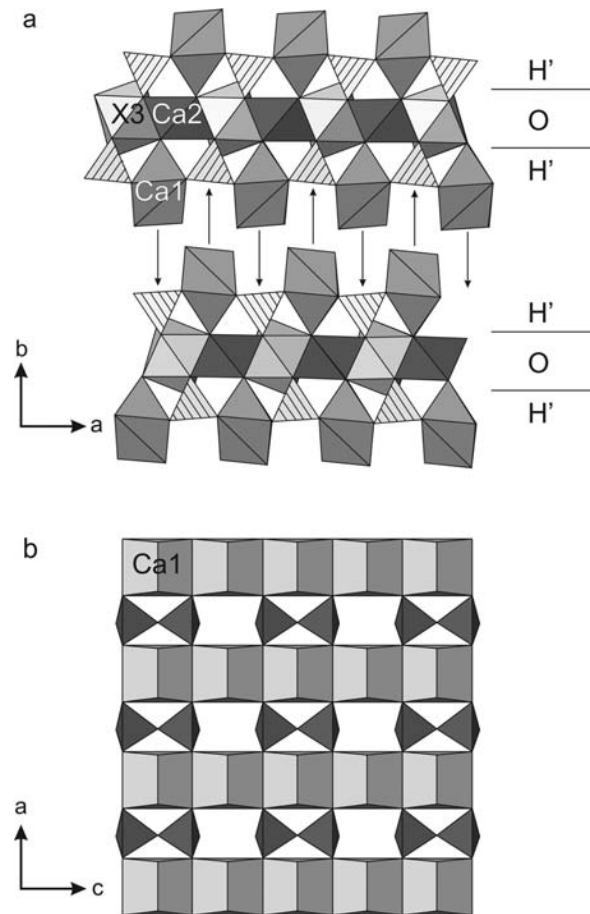


FIGURE 5. Dovyrenite (and rinkite) interpreted as a heterophyllosilicate: (a) splitting of the tobermorite Ca1 layer to form two H' sheets (silicon tetrahedra are hatched); (b) single-H' sheet of Ca1 sevenfold-coordinated polyhedra and disilicate groups, viewed along the b-axis.

TABLE 7. Comparison of cation site occupancies in rinkite (Galli and Alberti 1971; Rastsvetaeva et al. 1991) and dovyrenite (this study)

	Octahedral			7-coordinated				8-coordinated
	Ti	M1	M2	M3	M4	M5	M6	Na
Rinkite (Rastsvetaeva et al. 1991)		0.3 Ca 0.7 Na	0.3 Ca 0.7 Na	0.8 Ca 0.2 RE	0.7 Ca 0.3 RE	0.8 Ca 0.2 RE	0.8 Ca 0.2 RE	
Rinkite (Galli and Alberti 1971)	M1	M3			M4 and M5			M2
	0.52 Ti	0.759 Na			0.685 Ca			0.66 Na
	0.33 Nb	0.219 Ca			0.262 Ce			0.19 Ca
	0.09 Al	0.022 K			0.023 Fe			0.02 K
	0.07 Zr				0.020 Mg			0.13 □
					0.010 Th			
Dovyrenite	X3	Ca2			Ca1			X3
	0.5 Zr	0.36 Ca			1.0 Ca			0.5 Ca

ing in the tetrahedral sheet.

Although the interpretation of rinkite (and dovyrenite) as heterophyllosilicate (Christiansen and Rønsbo 2000; Sokolova 2006) is formally correct, it neglects the existence of the modular character of these minerals because the content of the dense tobermorite Ca-polyhedral layer is split into two separate H'-sheets (Fig. 5). Half of Ca of the tobermorite layer is assigned to each of the H'-sheets. Within the H'-sheets sevenfold-coordinated Ca substitutes on two different positions: (1) it replaces a disilicate unit in a mica-like sheet of tetrahedra; (2) it also occupies a peripheral cation site (Sokolova 2006). For this reason there are ribbons [along *c* in dovyrenite, and along *a* in rinkite (Galli and Alberti 1971)] of edge-sharing CaO₇ polyhedra where peripheral Ca alternates with Ca replacing Si₂O₇ units. The two adjacent H'-sheets are tightly linked together by common edges of the upper and lower Ca polyhedra and by shared edges between Si tetrahedra and Ca polyhedra (Fig. 5).

To establish a distinct structure topology for a specific chemical composition, Sokolova (2006) analyzed TS (titanium silicate) blocks in titanium disilicate minerals. These are three-layered structures consisting of an O-sheet (trioctahedral sheet in mica) and two heteropolyhedral H-sheets. Among her 24 analyzed examples of known structure and chemical composition, Sokolova (2006) also includes rinkite. However, dovyrenite, if its structure were known at the time of her study, would have been excluded because of the octahedral vacancies in the O-sheet, which does not fulfil the postulated constraint of a fully occupied trioctahedral mica sheet.

ACKNOWLEDGMENTS

T.A. acknowledges financial support by the Swiss National Science Foundation, grant 200020-112198 "Crystal Chemistry of Minerals."

REFERENCES CITED

- Bellezza, M., Franzini, M., Larsen, A.O., Merlino, S., and Perchiazzi, N. (2004) Grenmarite, a new member of the götzenite-seidozerite-rosenbuschite group from the Langesundsfjord district, Norway: definition and crystal structure. *European Journal of Mineralogy*, 16, 971–978.
- Brown, I.D. and Altermatt, D. (1985) Bond-valence parameters obtained from a systematic analysis of the inorganic crystal structure database. *Acta Crystallographica*, B41, 244–247.
- Bruker (1997) SHELXTL, Version 5.1. Bruker AXS Inc., Madison, Wisconsin, U.S.A.
- (1999) SAINT+, Version 6.02. Bruker AXS Inc., Madison, Wisconsin, U.S.A.
- Christiansen, C.C. and Rønsbo, J.G. (2000) On the structural relationship between götzenite and rinkite. *Neues Jahrbuch für Mineralogie—Monatshefte*, 2000, 496–506.
- Ferraris, G., Khomyakov, A.P., Belluso, E., and Soboleva, S.V. (1997) Polysomatic relationships in some titanosilicates occurring in the hyperagpaitic alkaline rocks of the Kola Peninsula, Russia. *Proceedings from the 30th International Geological Congress*, 16, 17–27.
- Ferraris, G., Makovicky, E., and Merlino, S. (2004) Crystallography of modular materials, 15, 370 p. IUCr Monographs on Crystallography, Oxford University Press, New York.
- Galli, E. and Alberti, A. (1971) The crystal structure of rinkite. *Acta Crystallographica*, B27, 1277–1284.
- Galuskina, E.V., Pertsev, N.N., Armbruster, T., Kadiyski, M.K., Zadov, A.E., Galuskina, I.O., Dzierzanowski, P., Wrzalik, R., and Kislov, E.B. (2007) Dovyrenite, Ca₄ZrSi₄O₁₄(OH)₄—a new mineral from skarned carbonate xenoliths in basic-ultrabasic rocks of the Dovyren massif, Northern Baikal region, Russia. *Mineralogia Polonica*, 31, 1–21.
- Gibbs, G.V. (1982) Molecules as models for bonding in silicates. *American Mineralogist*, 67, 421–450.
- Gnos, E. and Armbruster, T. (2000) Kinoshaltite, Ba(Mg)₃(Al₂Si₂)O₁₀(OH,F)₂, a brittle mica from a manganese deposit in Oman: Paragenesis and crystal chemistry. *American Mineralogist*, 85, 242–250.
- Gottardi, G. (1966) X-Ray crystallography of rinkite. *American Mineralogist*, 51, 1529–1535.
- Gurulev, S.A. (1983) Conditions of mafic differential intrusion formation. Nauka, Moscow (in Russian).
- Hoffmann, C. and Armbruster, T. (1997) Clinotobermorite, Ca₅[Si₃O₈(OH)]₂·4H₂O—Ca₅[Si₄O₁₇]·5H₂O, a natural C-S-H (I) type cement mineral. Determination of the substructure. *Zeitschrift für Kristallographie*, 212, 864–873.
- Kislov, E.V. (1998) Yoko-Dovyren differential massif. Ulan-Ude, Izd. Buryatskogo Nauchnogo Centra (in Russian).
- Konnikov, E.G. (1986) Differential hyperbasite-basite complexes of Zabaikalie Pre-Cambrian, 217 p. Novosibirsk, Nauka (in Russian).
- Li, D.Y., Simonov, V.I., and Belov, N.V. (1965) The crystal structure of rinkite Na(Na,Ca)₄(Ca,Ce)₄(Ti,Nb)₂[Si₂O₇]₂(O,F)₂. *Kristallografiya, Doklady Akademii Nauk SSSR*, 162(6), 1288–1291 (in Russian).
- Merlino, S., Bonaccorsi, E., and Armbruster, T. (1999) Tobermorites: Their real structure and order-disorder (OD) character. *American Mineralogist*, 84, 1613–1621.
- (2000) The real structures of clinotobermorite and tobermorite 9 Å: OD character, polytypes, and structural relationships. *European Journal of Mineralogy*, 12, 411–429.
- (2001) The real structure of tobermorite 11 Å: Normal and anomalous forms, OD character and polytypic modifications. *European Journal of Mineralogy*, 13, 577–590.
- Pertsev, N.N., Konnikov, E.G., Kislov, E.V., Orsoev, D.A., and Nekrasov, A.N. (2003) Merwinite-facies magnesian skarns in xenoliths from dunite of the Dovyren layered intrusion. *Petrologiya*, 11(5), 464–475 (in Russian).
- Petersen, O.V., Rønsbo, J.G., and Leonardsen, E.S. (1989) Nacareniobsite-(Ce), a new mineral species from the Ilmaussaq alkaline complex, South Greenland, and its relation to mosandrite and the rinkite series. *Neues Jahrbuch für Mineralogie—Monatshefte*, 1989, 84–96.
- Rastsvetaeva, R.K., Borutskii, B.E., and Shlyukova, Z.V. (1991) Crystal structure of Hibbing rinkite. *Soviet Physics Crystallography*, 36(3), 349–351.
- Simonov, V.I. and Belov, N.V. (1968) Characteristics of the crystal structure of rinkite. *Soviet Physics Crystallography*, 12(5), 740–744.
- Sokolova, E. (2006) From structure topology to chemical composition. I. Structural hierarchy and stereochemistry in titanium disilicate minerals. *The Canadian Mineralogist*, 44, 1273–1330.
- Taylor, H.F.W. (1959) The dehydration of tobermorite. *Clays and Clay Minerals*, 6, 101–109.
- Wenzel, Th., Baumgartner, L.P., Brüggemann, G.E., Konnikov, E.G., and Kislov, E.V. (2002) Partial melting and assimilation of dolomitic xenoliths by mafic magma: The Ioko-Dovyren intrusion (North Baikal Region, Russia). *Journal of Petrology*, 43, 2049–2074.
- Wilson, A.J.C. (1992) *International Tables for Crystallography*, Vol. C, Tables 6.1.1.4 (p. 500–502), 4.2.6.8 (p. 219–222), and 4.2.4.2 (p. 193–199), Kluwer Academic Publishers, Dordrecht.
- Zadov, A.E., Pertsev, N.N., Belakovskiy, D.I., Chukanov, N.V., and Kuznecova, O. Ju. (2004) Foshagite and hellebrandite in xenoliths from Yoko-Dovyrensky Massif (Transbaikalia). *Proceedings of the Russian Mineralogical Society*, 2004, 1, 73–83 (in Russian).

MANUSCRIPT RECEIVED APRIL 12, 2007

MANUSCRIPT ACCEPTED OCTOBER 8, 2007

MANUSCRIPT HANDLED BY SERGEY KRIVOVICHEV